

Non-linear adaptive tracking control for quadrotor aerial robots under uncertain dynamics

Yen-Chen Liu | Tsung-Wei Ou

Department of Mechanical Engineering, National Cheng Kung University, Tainan, Taiwan

Correspondence

Yen-Chen Liu, Department of Mechanical Engineering, National Cheng Kung University, Tainan 70101, Taiwan.

Email: yliu@mail.ncku.edu.tw

Funding information

Ministry of Science and Technology, Taiwan, Grant/Award Numbers: MOST 109-2636-E-006-019, MOST 108-2636-E-006-007

Abstract

This paper presents the design, analysis, and implementation of an adaptive backstepping controller for underactuated quadrotors to track time-varying trajectories with parameter uncertainties. Quadrotor systems are subject to complicated non-linearity and coupling dynamics, so the ignorance of parameter uncertainties may cause performance degradation and even instability. With the concept of nominal input, the uncertain mass and inertia are decoupled from the lifting force and moment torque. By utilizing the backstepping technique, the design procedure with adaptive laws for dynamic parameters is proposed to ensure stability and convergence of tracking errors to the origin asymptotically. The proposed control scheme is extended to control a quadrotor with velocity motor input while the motor coefficients and geometric parameters are handled by the adaptive laws. A trajectory generation for the proposed adaptive tracking controller is addressed subsequently. The proposed controller requires only the position and orientation of the quadrotor with the twice-differentiable trajectories, while previous work demanded acceleration information. Simulation and experimental results are illustrated to show the efficacy of tracking performance for object transportation.

1 | INTRODUCTION

Quadrotor aerial robots, with the advantages of higher mobility, agility, flexibility, have becoming a significant and promising research direction in the robotics and control communities [1, 2]. Moreover, the academic and industrial fields experience a substantial increasing of interest in quadrotor systems [3–5]. With the extensive utility, quadrotor systems have been accomplished in various applications, such as object transportation, agricultural mapping, disaster monitoring, search and rescue mission, and military surveillance [1, 2, 5]. The studies of quadrotor systems to track a time-varying trajectory with respect to uncertain physical parameters and environmental disturbances is the major research focus in both theoretical development and practical implementation [6, 7].

Although quadrotor systems have the excellence in vertical takeoff and landing (VTOL) with simple mechanical design, the non-linear, strong coupling, and underactuated characteristics make the development of control algorithms more crucial than grounded mobile robots. Over the past years, researchers have

paid significant attention in proposing efficient control schemes for quadrotor systems by PID controller [8, 9], feedback linearization [10, 11], model predictive control [12], geometric control [2], fuzzy control [13], and sliding mode control [14, 15]. The altitude and position tracking control for linearized quadrotor systems with wind gusts is addressed by model predictive control [12]. Recently, a geometric controller for quadrotors to transport a cable-suspended rigid body was studied to ensure the position and attitude tracking in the presence of uncertainties [2].

Additionally, backstepping control has been demonstrated a powerful non-linear control method for underactuated dynamics. There have been significant studies focusing on trajectory tracking control of quadrotors via backstepping [14, 16–20]. By considering the quadrotor system as a three-interconnected subsystems, an underactuated subsystem, a fully-actuated subsystems, and a propeller subsystem, a full-state backstepping technique was presented in [15, 19] to guarantee position and yaw angle tracking. The backstepping control was subsequently extended to quadrotor systems with sliding mode

This is an open access article under the terms of the [Creative Commons Attribution](https://creativecommons.org/licenses/by/4.0/) License, which permits use, distribution and reproduction in any medium, provided the original work is properly cited.

© 2021 The Authors. *IET Control Theory & Applications* published by John Wiley & Sons Ltd on behalf of The Institution of Engineering and Technology

technique [14], optimization [21], and disturbance observer [17]. However, most of the approaches was proposed by assuming that system parameters are correctly known in prior. The requirement of pre-estimation for the system parameters could not ensure real-time responses to sudden changes in structure and environment in practice.

To deal with uncertainties due to system parameters, aerodynamics, and disturbances, several control laws have been presented recently [4, 7, 22–25]. The adaptive self-tuning regulator was studied with proportional-integral (PI) controller to ensure quadrotor tracking subject to uncertain parameters [6]. A neural-network-based adaptive control was presented to cope with parameter uncertainties in trajectory tracking for a quadrotor system [23]. The mass variation and wind disturbances was addressed by utilizing a fuzzy wavelet neural network approach [4]. The disturbance and modelling uncertainties have been studied via the design of an observer in [17] and a projection-based adaptive scheme in [24]. Although these methods can well-address some uncertainties, the physical parameters that would degrade system performance and even threaten the stability were not taken into account carefully. Therefore, the control technique requiring no information of physical parameters demand further investigation.

Physical parameters of a quadrotor are usually difficult to obtain off-line because the value of mass and inertia could be varying with respect to the applications in object-picking tasks and cooperative transportation [6]. Several off-line measurements are utilized widely to obtain the physical parameters, for example computer-aided model, test-rig platform, or system identifications [3, 26, 27]. However, the parameter uncertainties resulting from different payload in various flight missions is unpractical to measure precisely during each flight. Imprecise measurements of dynamic parameters or suddenly attaching/detaching objects during flight operation would cause unexpectedly falling down or flying off. Consequently, the major challenge of controlling quadrotors, due to the inherent instability and complexity of the dynamic model, is in the development of an efficient algorithm independent to the knowledge of physical parameters. Thus, the position/attitude tracking control for quadrotor systems under mass, inertia, or even motor coefficient uncertainties is still an open problem for the studies of quadrotors. More importantly, when an object is attached to and detached from the quadrotor, the quadrotor aerial robot would fly away or stall if the dynamic uncertainties are not well-addressed in the control algorithm.

This paper presents an adaptive backstepping control algorithm for quadrotors to track a predefined trajectory subject to dynamic uncertainties. With the design of nominal input, the mass and rotational inertia are decoupled from the lifting force and moment torque, so that adaptive laws can be designed to cope with uncertain parameters. Different from the previous method [15], the entire quadrotor system is divided into four subsystems, which are position underactuated subsystems and three-Euler-angle subsystems. Each of the subsystem is utilized to design the controller via backstepping and adaptive laws for uncertain mass and inertia. Lyapunov theorem is applied to

study the boundedness of estimated parameters and the asymptotic convergence of the tracking errors to the origin. For the velocity control input, the uncertainties from coefficients of lifting force and moment torque, and geometric parameters can be handled by the modified adaptive laws. Furthermore, a trajectory generation of the proposed adaptive backstepping control is presented for both the torque input and velocity input scenarios. This paper illustrates simulation and experimental results to show the efficiency of the proposed adaptive backstepping algorithms.

The preliminary results of this work were presented in [18], where the basic design procedure of the adaptive backstepping controller and numerical examples were addressed. We extend these works by elaborating the complete theoretical analysis and extension to the control algorithm for velocity input with uncertain motor lifting force and moment coefficients. Moreover, the trajectory generation for the presented adaptive backstepping control is stated so that the quadrotor system has a feasible desired trajectory. The contributions of this paper are summarized as follows: (1) a backstepping-based adaptive control is proposed for quadrotor systems to track time-varying trajectories when the system parameters, mass and inertia, are unknown; nevertheless, dynamic parameters are required in [9, 28] for regulation and in [8, 29, 30] for trajectory tracking, respectively; (2) the proposed adaptive tracking control is transferred to velocity control input by taking the uncertainties of motor coefficients in lifting force and moment torque, and geometric parameter into consideration; (3) a trajectory generation for both the scenarios of torque input and velocity input scenarios is presented based on the proposed adaptive backstepping controller; (4) simulation and experimental results are presented, and the proposed control algorithms could be extended to quadrotor systems in cable-suspended load, aerial transportation, cooperative transportation, and aerial manipulation.

This paper is organized as follows. The preliminaries and modelling are introduced in Section 2, which is followed by the design procedure of backstepping and theoretical results for adaptive tracking control in Section 3. Numerical examples and experiments for adaptive backstepping tracking control with parameter uncertainties are discussed in Sections 4 and 5. Finally, Section 6 summarizes the results and discusses future research directions.

2 | QUADROTOR MODELLING AND CONTROL OBJECTIVE

2.1 | Quadrotor kinematics/dynamics

The kinematics and dynamics of a quadrotor system, as illustrated in Figure 1, are addressed in this section. With the assumption of six-DoF (degree-of-freedom) rigid body, the centre of mass of the quadrotor on the body frame $\{B\}$ with respect to the initial frame of reference $\{W\}$ is denoted by $\eta = [x, y, z]^T \in \mathbb{R}^3$. The Euler angles of the quadrotor with respect to the initial frame $\{W\}$ is described by $\Theta = [\phi, \theta, \psi]^T \in \mathbb{R}^3$.

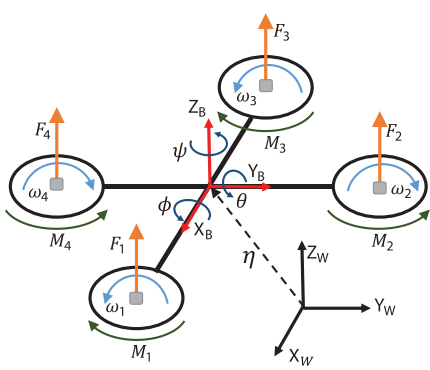


FIGURE 1 Quadrotor coordinates and motor forces/moment acting on the quadrotor frame

Hence, we have the quadrotor generalized coordinates as $\zeta = [x, y, z, \phi, \theta, \psi]^T \in \mathbb{R}^6$, where ϕ is the roll angle around the x -axis, θ is the pitch angle around the y -axis, and ψ is the yaw angle around the z -axis.

Thus, the velocity relationship from the initial frame $\{W\}$ to the body frame $\{B\}$ can be formulated as

$$\varpi = \Xi_T^R \dot{\zeta}, \quad (1)$$

where $\varpi = [V_B^T, \Omega_B^T]^T = [u, v, w, p, q, r]^T \in \mathbb{R}^6$ contains the linear velocity $V_B = [u, v, w]^T \in \mathbb{R}^3$ and angular velocity $\Omega_B = [p, q, r]^T \in \mathbb{R}^3$ with respect to the body frame $\{B\}$. In (1), Ξ_T^R is the transformation matrix that is described by

$$\Xi_T^R = \begin{bmatrix} R^T & 0_{3 \times 3} \\ 0_{3 \times 3} & T \end{bmatrix}, \quad (2)$$

where $0_{n \times n} \in \mathbb{R}^{n \times n}$ is a zero matrix. The Euler angles z - x - y are utilized to model the quadrotor rotation; thus, the rotational matrix in (2) is defined as $R = R_{z\psi} R_{x\phi} R_{y\theta}$ that

$$R = \begin{bmatrix} c\theta c\psi - s\phi s\theta s\psi & -c\phi s\psi & s\theta c\psi + s\phi c\theta s\psi \\ c\theta s\psi + s\phi s\theta c\psi & c\phi c\psi & s\theta s\psi - s\phi c\theta c\psi \\ -c\phi s\theta & s\phi & c\phi c\theta \end{bmatrix}, \quad (3)$$

where $c\phi$ and $s\phi$ denote $\cos(\phi)$ and $\sin(\phi)$, respectively for $\phi = \{\psi, \theta, \phi\}$. Furthermore, the translational matrix $T \in \mathbb{R}^{3 \times 3}$ in (2) from $\dot{\Theta} = [\dot{\phi}, \dot{\theta}, \dot{\psi}]^T$ to $\Omega_B = [p, q, r]^T$ is given by [5]

$$T = \begin{bmatrix} c\theta & 0 & -c\phi s\theta \\ 0 & 1 & s\phi \\ s\theta & 0 & c\phi c\theta \end{bmatrix}. \quad (4)$$

In the modelling, the Euler angles are assumed to be bounded such that $-\pi/2 < \phi < \pi/2$, $-\pi/2 < \theta < \pi/2$, and $-\pi < \psi < \pi$, and operated in small angles so that the transformation matrix T is non-singular.

With the Euler-Lagrangian approaches, the quadrotor dynamics can be expressed as

$$\begin{bmatrix} m_q I_{3 \times 3} & 0_{3 \times 3} \\ 0_{3 \times 3} & J_q \end{bmatrix} \begin{bmatrix} \dot{V}_B \\ \dot{\Omega}_B \end{bmatrix} + \begin{bmatrix} \Omega_B \times (m_q V_B) \\ \Omega_B \times (J_q \Omega_B) \end{bmatrix} = \begin{bmatrix} F_{ext} \\ \tau_{ext} \end{bmatrix}, \quad (5)$$

where $I_{n \times n} \in \mathbb{R}^{n \times n}$ is an identity matrix, m_q denotes the mass of the quadrotor, $J_q \in \mathbb{R}^{3 \times 3}$ denotes the inertia matrix of the quadrotor with respect to the body frame $\{B\}$, $F_{ext} = F_T + F_g \in \mathbb{R}^3$ is the exerted force, $\tau_{ext} = \tau = [\tau_x, \tau_y, \tau_z]^T \in \mathbb{R}^3$ is the torque applied on the quadrotor. By denoting $a_3 = [0, 0, 1]^T$, the terms in the thrust force F_{ext} are given as $F_T = [0, 0, F]^T := F a_3 \in \mathbb{R}^3$ with $F \in \mathbb{R}$ as the total thrust force which applies on the z -axis of the quadrotor, and $F_g = R^T [0, 0, -m_q g]^T := -m_q g R^T a_3 \in \mathbb{R}^3$ as the gravitational force vector.

Consequently, the dynamic model, without the influence of aerodynamic/propeller effects, can be described by [3, 31]

$$\begin{cases} m_q \ddot{\eta} = F R a_3 - m_q g a_3 \\ J_q \dot{\Omega}_B = \tau - \Omega_B \times J_q \Omega_B. \end{cases} \quad (6)$$

If the quadrotor carries an object via gripper or a manipulator, the mass and rotational inertia matrix of the entire quadrotor system would be influenced by the object. By considering the mass and inertia of the object are constant and denoted by m_o and $J_o \in \mathbb{R}^3$, a diagonal matrix, then the dynamic of the quadrotor can be modified and given as

$$\begin{cases} m \ddot{\eta} = F R a_3 - m g a_3 \\ J \dot{\Omega}_B = \tau - \Omega_B \times J \Omega_B, \end{cases} \quad (7)$$

where $m = m_q + m_o$ and $J = J_q + J_o$. As the quadrotor structure is symmetric, the inertia matrix is given as a diagonal matrix such that $J = \text{diag}\{I_x, I_y, I_z\}$, where I_x , I_y , and I_z are the diagonal elements in the inertia matrix J of the quadrotor and attached object. Under the assumption of operation in small angels, Ω_B can be approximated by $\dot{\Theta} = [\dot{\phi}, \dot{\theta}, \dot{\psi}]^T$. Hence, the dynamic equations becomes [26, 32]

$$\ddot{x} = \frac{F}{m} (s\theta c\psi + s\phi c\theta s\psi), \quad (8)$$

$$\ddot{y} = \frac{F}{m} (s\theta s\psi - s\phi c\theta c\psi), \quad (9)$$

$$\ddot{z} = \frac{F}{m} c\phi c\theta - g, \quad (10)$$

$$\ddot{\phi} = \frac{I_y - I_z}{I_x} \dot{\theta} \dot{\psi} + \frac{\tau_x}{I_x}, \quad (11)$$

$$\ddot{\theta} = \frac{I_z - I_x}{I_y} \dot{\phi} \dot{\psi} + \frac{\tau_y}{I_y}, \quad (12)$$

$$\ddot{\psi} = \frac{I_x - I_y}{I_z} \dot{\phi} \dot{\theta} + \frac{\tau_z}{I_z}. \quad (13)$$

A quadrotor system is actuated by the rotational speed of the four motors which can be converted to the control input force F and moment torque τ [5, 26]. Therefore, the force generated from each of the motor can be obtained by $F_i = k_F \omega_i^2$, where F_i are the lifting force of the i^{th} motor, ω_i is the motor speed of the i^{th} motor, and $k_F > 0$ as the lifting force coefficient. For the moment resulting from the motor, we have that $M_i = k_M \omega_i^2$ for $i = 1, 2, 3, 4$, where M_i is the moment from the i^{th} motor, and $k_M > 0$ is the coefficient of the motor moment. By denoting d as the distance from the rotor axes to the quadrotor epicentre, the control input (7) $F = \sum_{i=1}^4 F_i$, $\tau_x = d(F_2 - F_4)$, $\tau_y = d(F_3 - F_1)$, and $\tau_z = \sum_{i=1}^4 (-1)^{i+1} M_i$. Hence, the relationship between the motor speed to the control inputs is given as

$$\begin{bmatrix} F \\ \tau_x \\ \tau_y \\ \tau_z \end{bmatrix} = \begin{bmatrix} k_F & k_F & k_F & k_F \\ 0 & dk_F & 0 & -dk_F \\ -dk_F & 0 & dk_F & 0 \\ -k_M & k_M & -k_M & k_M \end{bmatrix} \begin{bmatrix} \omega_1^2 \\ \omega_2^2 \\ \omega_3^2 \\ \omega_4^2 \end{bmatrix}. \quad (14)$$

Therefore, with the design of control force and moment, F and τ , the motor speed can be obtained with the knowledge of d , k_F , and k_M to control the motion of a quadrotor system.

2.2 | Control objective and formulation

In the quadrotor model, the mass m and moment of inertia I_x , I_y , and I_z are basically unknown to the controller, especially during the transportation of an object. The uncertain or inaccurate mass and inertia information would degrade the tracking performance of a quadrotor system. Although these parameters could be obtained experimentally, or using CAD model, the traditional methods are not useful for unknown object in aerial transportation or manipulation. Therefore, the main objective of this paper is to design a control technique so that the quadrotor system can track a time-varying trajectory without the knowledge of the dynamic parameters, m and J .

Since the parameter uncertainties have significantly influence to tracking performance and even stability of a quadrotor, the main purpose of this paper is to develop control algorithms so that the quadrotor system can track a desired trajectory without the knowledge of dynamic, that is m , I_x , I_y , and I_z are unknown to the controller. The objective of this paper is to propose an adaptive controller so that the convergence of the positions $\eta(t)$ and Euler angle $\phi(t)$, $\theta(t)$, $\psi(t)$, to a desired trajectories $\{\eta_d(t), \psi_d(t)\} = \{x_d(t), y_d(t), z_d(t), \psi_d(t)\} \in \mathbb{R}^4$, respectively, are guaranteed. It is noted that the convergence of roll and pitch angles to the reference angles, whose desired trajectories are obtained from $\{x_d(t), y_d(t), z_d(t), \psi_d(t)\}$ and denoted by $\phi_d(t)$ and $\theta_d(t)$, respectively, are also guaranteed with the controller. The trajectory generation for the quadrotor system will be addressed subsequently in Section 3.4.

For the proposed non-linear adaptive control for quadrotor tracking with uncertain system parameters, the aforementioned assumptions are summarized and described in the following:

Assumption 1. The quadrotor aerial robot is a six-DoF rigid body with the centre of mass located at the geometric centre.

Assumption 2. The roll and pitch angles, ϕ and θ , of the quadrotor aerial robot are operated in small angles.

Assumption 3. The quadrotor aerial robot is controlled while neglecting the aerodynamic/propeller effects.

Assumption 4. The desired positions and Euler angles in the trajectory tracking control are twice differentiable.

3 | ADAPTIVE BACKSTEPPING CONTROL

3.1 | Design procedure

By observing the dynamic models, (8) to (13), we obtain that the input force F and torque τ_x , τ_y , τ_z are divided by either the mass m or the rotational inertia I_x , I_y , I_z . Therefore, to handle the dynamic parameters, the thrust force F and moment torque τ are rewritten with the nominal inputs that

$$F = m\bar{F}, \tau_x = I_x\bar{\tau}_x, \tau_y = I_y\bar{\tau}_y, \tau_z = I_z\bar{\tau}_z, \quad (15)$$

where \bar{F} , $\bar{\tau}_x$, $\bar{\tau}_y$, $\bar{\tau}_z$ are called the nominal inputs of the quadrotor system without mass/inertia. Hence, the control inputs are designed under the definition of nominal inputs and the corresponding dynamic parameters. If there are dynamic uncertainties in the quadrotor system, the estimation of dynamic parameters can be utilized in the control input such that

$$F = \hat{m}\bar{F}, \tau_x = \hat{I}_x\bar{\tau}_x, \tau_y = \hat{I}_y\bar{\tau}_y, \tau_z = \hat{I}_z\bar{\tau}_z, \quad (16)$$

where \hat{m} , \hat{I}_x , \hat{I}_y , and \hat{I}_z denote the estimates of m , I_x , I_y , and I_z , respectively. Consequently, under the formulation (16), the uncertain dynamics can be tackled separately by the design of control inputs. To cope with dynamic uncertainties in the studies of quadrotor trajectory, an adaptive backstepping control [33] is presented. The following states $\xi_1 = \eta$, $\xi_2 = \dot{\eta}$, $\xi_3 = \phi$, $\xi_4 = \dot{\phi}$, $\xi_5 = \theta$, $\xi_6 = \dot{\theta}$, $\xi_7 = \psi$, and $\xi_8 = \dot{\psi}$, where $\xi_1, \xi_2 \in \mathbb{R}^3$ and $\xi_j \in \mathbb{R}$ for $j = 3, \dots, 8$, are considered for the quadrotor system. For the design of the control law, the quadrotor system is divided into four subsystems, and the design procedure are presented subsequently.

Step 1: Let the first virtual system of the quadrotor be given as $\dot{\xi}_1 = v_1$. By considering $V_1 = e_1^T e_1 / 2$ as the Lyapunov function candidate with $e_1 = \xi_1 - \eta_d$ as the position tracking error, the time-derivative of V_1 gives that $\dot{V}_1 = e_1^T \dot{e}_1 = e_1^T (\dot{\xi}_1 - \dot{\eta}_d) = e_1^T (v_1 - \dot{\eta}_d)$. Thus, the subsystem of e_1 can be

stabilized by designing the first virtual input as $v_1 = \dot{\eta}_d - k_1 e_1$ with a positive control gain k_1 . Consequently, we get $\dot{V}_1 = -k_1 e_1^T e_1 \leq 0$.

Step 2: By considering the position subsystem of the quadrotor ($\xi_1 = \eta$), as described in (7), we have

$$\begin{cases} \dot{\xi}_1 = \xi_2 \\ \dot{\xi}_2 = -ga_3 + Ra_3 F/m. \end{cases} \quad (17)$$

By designing the tracking error $e_2 = \xi_2 - v_1$, the derivatives of e_1 and e_2 with the design of v_1 and (7) gives that

$$\begin{cases} \dot{e}_1 = \dot{\xi}_1 - \dot{\eta}_d = \xi_2 - \dot{\eta}_d + v_1 - v_1 = e_2 - k_1 e_1 \\ \dot{e}_2 = \dot{\xi}_2 - \dot{v}_1 = -ga_3 + Ra_3 F/m - (\ddot{\eta}_d - k_1 \dot{e}_1). \end{cases} \quad (18)$$

Hence, the augmented Lyapunov function is given as

$$V_2 = \frac{1}{2} e_1^T e_1 + \frac{1}{2} e_2^T e_2 + \frac{\tilde{m}^2}{2\gamma_m m}, \quad (19)$$

where $\tilde{m} = m - \hat{m}$ denotes the estimation error between \hat{m} and the actual m , and $\gamma_m \in \mathbb{R}$ is a positive gain of the adaptive law that will be presented subsequently. Since m is a constant during an operation, $\dot{\tilde{m}} = -\dot{\hat{m}}$. Thus, the time-derivative of V_2 along the trajectories of (18) is given as

$$\begin{aligned} \dot{V}_2 = & e_1^T (e_2 - k_1 e_1) + e_2^T \left(-ga_3 + \frac{F}{m} Ra_3 - (\ddot{\eta}_d - k_1 \dot{e}_1) \right) \\ & - \frac{\tilde{m}}{\gamma_m m} \dot{\hat{m}}. \end{aligned} \quad (20)$$

From the definition of the nominal input $F = \hat{m} \bar{F}$ and estimate error \tilde{m} in (16), the term F/m can be rewritten as

$$F/m = \bar{F} - \bar{F} \tilde{m}/m. \quad (21)$$

By denoting $R_f = Ra_3 \in \mathbb{R}^3$, \dot{V}_2 can be written as

$$\begin{aligned} \dot{V}_2 = & e_1^T (e_2 - k_1 e_1) + e_2^T (-ga_3 + \bar{F} R_f - \ddot{\eta}_d + k_1 \dot{e}_1) \\ & - \frac{\tilde{m}}{\gamma_m m} (\hat{m} + \gamma_m \bar{F} e_2^T R_f). \end{aligned} \quad (22)$$

Furthermore, we can design the adaptive law for $\dot{\hat{m}}$ as

$$\dot{\hat{m}} = -\gamma_m \bar{F} e_2^T R_f, \quad (23)$$

so that the time-derivative of V_2 becomes

$$\begin{aligned} \dot{V}_2 = & -k_1 e_1^T e_1 - k_2 e_2^T e_2 + \bar{F} e_2^T R_f \\ & + e_2^T (-ga_3 + \ddot{\eta}_d + k_1 \dot{e}_1 + e_1 + k_2 e_2). \end{aligned} \quad (24)$$

Therefore, we get $\dot{V}_2 = -k_1 e_1^T e_1 - k_2 e_2^T e_2$ if the last two terms in (24) are zero such that

$$\bar{F} e_2^T R_f = -e_2^T (-ga_3 + \ddot{\eta}_d + k_1 \dot{e}_1 + e_1 + k_2 e_2). \quad (25)$$

Since e_2 and R_f are vectors with the corresponding dimension, we further obtain the nominal input $\bar{F} \in \mathbb{R}$ as

$$\bar{F} = -\left(e_2^T R_f \right)^{-1} \left(e_2^T (-ga_3 + \ddot{\eta}_d + k_1 \dot{e}_1 + e_1 + k_2 e_2) \right). \quad (26)$$

Thus, the adaptive law (23) and the nominal input (26) guarantee that \dot{V}_2 is negative semi-definite so that e_1 , e_2 , and \hat{m} are bounded.

Step 3: Let's consider the second virtual system described by $\dot{\xi}_3 = v_3$. By considering $V_3 = e_3^2/2$ as the Lyapunov function candidate with $e_3 = \xi_3 - \phi_d$, the time-derivative of V_3 is expressed as $\dot{V}_3 = e_3 \dot{e}_3 = e_3 (\xi_3 - \phi_d) = e_3 (v_3 - \phi_d)$. By designing the virtual control input as $v_3 = \phi_d - k_3 e_3$, we get that the time-derivative of V_3 becomes $\dot{V}_3 = -k_3 e_3^2 \leq 0$.

Step 4: Consider the roll-angle-subsystem of the quadrotor system (11) as

$$\begin{cases} \dot{\xi}_3 = \xi_4 \\ \dot{\xi}_4 = \dot{\theta} \dot{\psi} (I_y - I_z)/I_x + \tau_x/I_x = \rho_\phi \xi_6 \xi_8 + \tau_x/I_x, \end{cases} \quad (27)$$

where $\rho_\phi := (I_y - I_z)/I_x$. By letting the tracking error be $e_4 = \xi_4 - v_3$, the time-derivative of e_3 and e_4 are

$$\begin{cases} \dot{e}_3 = \dot{\xi}_3 - \dot{\phi}_d = \xi_4 - \dot{\phi}_d + v_3 - v_3 = e_4 - k_3 e_3 \\ \dot{e}_4 = \dot{\xi}_4 - \dot{v}_3 = \rho_\phi \xi_6 \xi_8 + \tau_x/I_x - (\dot{\phi}_d - k_3 \dot{e}_3). \end{cases} \quad (28)$$

As the dynamic parameters I_x and ρ_ϕ are unknown to the controller, $\tilde{I}_x = I_x - \hat{I}_x$ and $\tilde{\rho}_\phi = \rho_\phi - \hat{\rho}_\phi$ are defined as the estimation errors. Next, the Lyapunov function for the roll angle subsystem is given as

$$V_4 = \frac{1}{2} e_3^2 + \frac{1}{2} e_4^2 + \frac{1}{2\gamma_\phi} \tilde{\rho}_\phi^2 + \frac{1}{2\gamma_x I_x} \tilde{I}_x^2, \quad (29)$$

where γ_ϕ and γ_x are the adaptive control gains. The time-derivative of V_4 along the trajectories of \dot{e}_3 and \dot{e}_4 in (57) gives that

$$\begin{aligned} \dot{V}_4 = & e_3 (e_4 - k_3 e_3) + e_4 \left(\rho_\phi \xi_6 \xi_8 + \frac{\tau_x}{I_x} - (\dot{\phi}_d - k_3 \dot{e}_3) \right) \\ & - \frac{\tilde{\rho}_\phi}{\gamma_\phi} \dot{\tilde{\rho}}_\phi - \frac{\tilde{I}_x}{\gamma_x I_x} \dot{\tilde{I}}_x. \end{aligned} \quad (30)$$

With the definition of \tilde{I}_x and the nominal inputs, we get $\tau_x/I_x = \bar{\tau}_x - \bar{\tau}_x \tilde{I}_x/I_x$. Hence, \dot{V}_4 can be written as

$$\begin{aligned} \dot{V}_4 = & e_3 (e_4 - k_3 e_3) + e_4 (\hat{\rho}_\phi \xi_6 \xi_8 + \bar{\tau}_x - \ddot{\phi}_d + k_3 \dot{e}_3) \\ & + \frac{\tilde{\rho}_\phi}{\gamma_\phi} (\gamma_\phi e_4 \xi_6 \xi_8 - \dot{\tilde{\rho}}_\phi) - \frac{\tilde{I}_x}{\gamma_x I_x} (\bar{\tau}_x e_4 + \dot{\tilde{I}}_x). \end{aligned} \quad (31)$$

By designing that $\dot{\hat{\rho}}_\phi = \gamma_\phi e_4 \xi_6 \xi_8$ and $\dot{\hat{I}}_x = -\gamma_x \bar{\tau}_x e_4$, we have

$$\dot{V}_4 = e_3(e_4 - k_3 e_3) + e_4(\hat{\rho}_\phi \xi_6 \xi_8 + \bar{\tau}_x - \dot{\phi}_d + k_3 e_3). \quad (32)$$

Subsequently, by designing the nominal input as $\bar{\tau}_x = -e_3 + \dot{\phi}_d - k_3 e_3 - \hat{\rho}_\phi \xi_6 \xi_8 - k_4 e_4$, the time-derivative of V_4 becomes $\dot{V}_4 = -k_3 e_3^2 - k_4 e_4^2 \leq 0$.

Step 5: Let's consider the third virtual system as $\dot{\xi}_5 = v_5$, where $v_5 \in \mathbb{R}$ is a virtual control input. With the design of the tracking error $e_5 = \xi_5 - \theta_d$, the time-derivative of the Lyapunov function candidate $V_5 = e_5^2/2$ results in $\dot{V}_5 = e_5 \dot{e}_5 = e_5(\dot{\xi}_5 - \dot{\theta}_d)$. Thus, the design of the virtual control input v_5 as $v_5 = \dot{\theta}_d - k_5 e_5$ with k_5 as a positive control gains leads to that $\dot{V}_5 = -k_5 e_5^2 \leq 0$.

Step 6: Thus, by considering the pitch-angle-subsystem (12), we get

$$\begin{cases} \dot{\xi}_5 = \xi_6 \\ \dot{\xi}_6 = \dot{\phi} \dot{\psi} (I_x - I_\infty) / I_y + \tau_y / I_y = \rho_\theta \xi_4 \xi_8 + \tau_y / I_y, \end{cases} \quad (33)$$

where $\rho_\theta = (I_\infty - I_x) / I_y$. By letting the tracking error as $e_6 = \xi_6 - v_5$, the time-derivative of the errors e_5 and e_6 are given by

$$\begin{cases} \dot{e}_5 = \dot{\xi}_5 - \dot{\theta}_d = \xi_5 - \dot{\theta}_d + v_5 - v_5 = e_6 - k_5 e_5 \\ \dot{e}_6 = \dot{\xi}_6 - \dot{v}_5 = \rho_\theta \xi_4 \xi_8 + \tau_y / I_y - (\ddot{\theta}_d - k_5 \dot{e}_5). \end{cases} \quad (34)$$

By considering the positive-definite Lyapunov function

$$V_6 = \frac{1}{2} e_5^2 + \frac{1}{2} e_6^2 + \frac{1}{2\gamma_\theta} \tilde{\rho}_\theta^2 + \frac{1}{2\gamma_y I_y} \tilde{I}_y^2, \quad (35)$$

where $\tilde{\rho}_\theta = \rho_\theta - \hat{\rho}_\theta$ and $\tilde{I}_y = I_y - \hat{I}_y$, the time-derivative of V_6 is given as $\dot{V}_6 = e_5 \dot{e}_5 + e_6 \dot{e}_6 + \frac{\tilde{\rho}_\theta}{\gamma_\theta} (-\dot{\hat{\rho}}_\theta) + \frac{\tilde{I}_y}{\gamma_y I_y} (-\dot{\hat{I}}_y)$. Similar to Step 4, we get $\tau_y / I_y = \bar{\tau}_y - \bar{\tau}_y \tilde{I}_y / I_y$; thus, \dot{V}_6 , along the trajectories of e_5 and e_6 in (34), becomes

$$\begin{aligned} \dot{V}_6 = & e_5 e_6 - k_5 e_5^2 + e_6 (\hat{\rho}_\theta \xi_4 \xi_8 + \bar{\tau}_y) + \frac{\tilde{\rho}_\theta}{\gamma_\theta} (\gamma_\theta e_6 \xi_4 \xi_8 - \dot{\hat{\rho}}_\theta) \\ & + \frac{\tilde{I}_y}{\gamma_y I_y} (\gamma_y \bar{\tau}_y e_6 + \dot{\hat{I}}_y). \end{aligned} \quad (36)$$

By proposing the adaptive laws as $\dot{\hat{\rho}}_\theta = \gamma_\theta e_6 \xi_4 \xi_8$, $\dot{\hat{I}}_y = -\gamma_y \bar{\tau}_y e_6$, and the nominal input as $\bar{\tau}_y = -k_6 e_6 - e_5 + \ddot{\theta}_d - k_5 \dot{e}_5 - \hat{\rho}_\theta \xi_4 \xi_8$, where k_6 is a positive control gain, we get $\dot{V}_6 = -k_6 e_6^2 - k_5 e_5^2 \leq 0$ which is negative semi-definite.

Step 7: Let's consider the fourth virtual system as $\dot{\xi}_7 = v_7$, where $v_7 \in \mathbb{R}$ is a virtual control input. By considering $e_7 = \xi_7 - \psi_d$ as the tracking error, the Lyapunov function candidate $V_7 = e_7^2/2$ yields $\dot{V}_7 = e_7 \dot{e}_7 = e_7(\dot{\xi}_7 - \dot{\psi}_d)$. Hence, the design of the virtual control input v_7 as $v_7 = \dot{\psi}_d - k_7 e_7$ with k_7 as a positive control gains gives that $\dot{V}_7 = -k_7 e_7^2 \leq 0$.

Step 8: Let's consider the yaw-angle-subsystem (13) as

$$\begin{cases} \dot{\xi}_7 = \xi_8 \\ \dot{\xi}_8 = \dot{\phi} \dot{\theta} (I_x - I_\infty) / I_y + \tau_z / I_z = \rho_\psi \xi_4 \xi_6 + \tau_z / I_z, \end{cases} \quad (37)$$

where $\rho_\psi = (I_x - I_\infty) / I_z$. By designing the tracking error as $e_8 = \xi_8 - v_7$, we get the time-derivative of errors that

$$\begin{cases} \dot{e}_7 = \dot{\xi}_7 - \dot{\psi}_d = \xi_8 - \dot{\psi}_d + v_7 - v_7 = e_8 - k_7 e_7 \\ \dot{e}_8 = \dot{\xi}_8 - \dot{v}_7 = \rho_\psi \xi_4 \xi_6 + \tau_z / I_z - (\dot{\psi}_d - k_7 e_7). \end{cases} \quad (38)$$

Next, we take the positive-definite Lyapunov function as

$$V_8 = \frac{1}{2} e_7^2 + \frac{1}{2} e_8^2 + \frac{1}{2\gamma_\psi} \tilde{\rho}_\psi^2 + \frac{1}{2\gamma_z I_z} \tilde{I}_z^2, \quad (39)$$

where $\tilde{\rho}_\psi = \rho_\psi - \hat{\rho}_\psi$ and $\tilde{I}_z = I_z - \hat{I}_z$. Analogous to the proof in Step 6, the time-derivative of V_8 becomes $\dot{V}_8 = -k_7 e_7^2 - k_8 e_8^2 \leq 0$ by considering the adaptive laws as $\dot{\hat{\rho}}_\psi = \gamma_\psi e_8 \xi_4 \xi_6$, $\dot{\hat{I}}_z = -\gamma_z \bar{\tau}_z e_8$, and the nominal control input as $\bar{\tau}_z = -\hat{\rho}_\psi \xi_4 \xi_6 + \dot{\psi}_d - k_7 \dot{e}_7 - e_7 - k_8 e_8$ with k_8 as positive control gain.

After addressing the design procedure, the stability analysis of the proposed adaptive backstepping control for quadrotor trajectory tracking is addressed in the next section.

3.2 | Stability analysis

The control input F , τ_x , τ_y , and τ_z with the consideration of adaptive laws for dynamic uncertainties m , I_x , I_y , I_z , $\rho_\phi = (I_y - I_\infty) / I_x$, $\rho_\theta = (I_z - I_\infty) / I_y$, and $\rho_\psi = (I_x - I_\infty) / I_z$ are addressed in the aforementioned eight steps. Let's define the tracking errors that $e_1(t) = \eta(t) - \eta_d(t)$, $e_2(t) = \dot{e}_1(t) + k_1 e_1(t)$, $e_3(t) = \phi(t) - \phi_d(t)$, $e_4(t) = \dot{e}_3(t) + k_3 e_3(t)$, $e_5(t) = \theta(t) - \theta_d(t)$, $e_6(t) = \dot{e}_5(t) + k_5 e_5(t)$, $e_7(t) = \psi(t) - \psi_d(t)$, and $e_8(t) = \dot{e}_7(t) + k_7 e_7(t)$, where $\eta_d(t) \in \mathbb{R}^3$ and $\phi_d(t), \theta_d(t), \psi_d(t) \in \mathbb{R}$ are twice differentiable desired trajectories. The stability and convergence of the position/orientation tracking errors for a quadrotor system subject to dynamic uncertainties are stated in the next theorem.

Theorem 1. Consider the quadrotor system described by (8)–(13). For the force and torque inputs given by (16) with the nominal control inputs as

$$\bar{F} = -(e_2^T R_f)^{-1} (e_2^T (-g a_3 + \ddot{\eta}_d + k_1 \dot{e}_1 + e_1 + k_2 e_2)), \quad (40)$$

$$\bar{\tau}_x = -e_3 - k_3 \dot{e}_3 - k_4 e_4 + \ddot{\phi}_d - \hat{\rho}_\phi \dot{\theta} \dot{\psi}, \quad (41)$$

$$\bar{\tau}_y = -e_5 - k_5 \dot{e}_5 - k_6 e_6 + \ddot{\theta}_d - \hat{\rho}_\theta \dot{\phi} \dot{\psi}, \quad (42)$$

$$\bar{\tau}_z = -e_7 - k_7 \dot{e}_7 - k_8 e_8 + \ddot{\psi}_d - \hat{\rho}_\psi \dot{\phi} \dot{\theta}, \quad (43)$$

and the adaptive laws for the uncertain parameters given as

$$\dot{\hat{m}} = -\gamma_m \bar{F} e_2^T R_f, \quad (44)$$

$$\dot{\hat{\rho}}_\phi = \gamma_\phi e_4 \dot{\theta} \dot{\psi}, \quad \dot{\hat{I}}_x = -\gamma_x \bar{\tau}_x e_4, \quad (45)$$

$$\dot{\hat{\rho}}_\theta = \gamma_\theta e_6 \dot{\phi} \dot{\psi}, \quad \dot{\hat{I}}_y = -\gamma_y \bar{\tau}_y e_6, \quad (46)$$

$$\dot{\hat{\rho}}_\psi = \gamma_\psi e_8 \dot{\phi} \dot{\theta}, \quad \dot{\hat{I}}_z = -\gamma_z \bar{\tau}_z e_8, \quad (47)$$

the quadrotor control system is stable, and the position/attitude tracking errors e_1, e_3, e_5, e_7 , and velocity tracking errors $\dot{e}_1, \dot{e}_3, \dot{e}_5, \dot{e}_7$ converge to the origin asymptotically.

Proof. Let's consider the positive-definite Lyapunov function candidate for the proposed quadrotor control system as $V = V_2 + V_4 + V_6 + V_8$. With the analyses in Section 3.1, the time-derivative of V along the trajectories of controller and adaptive laws gives that $\dot{V} = -k_1 e_1^T e_1 - k_2 e_2^T e_2 - k_3 e_3^T e_3 - k_4 e_4^T e_4 - k_5 e_5^T e_5 - k_6 e_6^T e_6 - k_7 e_7^T e_7 - k_8 e_8^T e_8$, which is negative semi-definite. The integral of \dot{V} from 0 to t results that $V(t) \leq V(0)$ and $V(t)$ has a finite limit as $t \rightarrow \infty$. Therefore, we get that $e_1, e_2, e_3, e_4, e_5, e_6, e_7, e_8, \hat{m}, \hat{I}_x, \hat{I}_y, \hat{I}_z, \hat{\rho}_\phi, \hat{\rho}_\theta$, and $\hat{\rho}_\psi$ are bounded. By taking the time-derivative of V again, we obtain

$$\begin{aligned} \ddot{V} = & -2k_1 e_1^T \dot{e}_1 - 2k_2 e_2^T \dot{e}_2 - 2k_3 e_3 \dot{e}_3 - 2k_4 e_4 \dot{e}_4 \\ & - 2k_5 e_5 \dot{e}_5 - 2k_6 e_6 \dot{e}_6 - 2k_7 e_7 \dot{e}_7 - 2k_8 e_8 \dot{e}_8. \end{aligned} \quad (48)$$

As e_1 and e_2 are bounded, $\dot{e}_1 \in \mathcal{L}_\infty$ from (18). Similarly, we have that \dot{e}_3, \dot{e}_5 , and $\dot{e}_7 \in \mathcal{L}_\infty$. Since $\dot{\eta}_d, e_1, \dot{e}_1, e_2$ are bounded, we obtain that \bar{F} is bounded by observing (40). Furthermore, we get that $F = \bar{F} \hat{m} \in \mathcal{L}_\infty$ as $\hat{m} \in \mathcal{L}_\infty$. From the position dynamics (8), (9), (10), F being bounded leads to that \ddot{x}, \ddot{y} , and \ddot{z} are bounded, so does $\ddot{\eta} \in \mathcal{L}_\infty$. Hence, $\ddot{e}_1 = \ddot{\eta} - \dot{\eta}_d$ is also bounded. By taking the time-derivative of e_2 , we obtain that $\dot{e}_2 = \ddot{e}_1 + k_1 \dot{e}_1$. Moreover, the boundedness of $\ddot{e}_1, \dot{e}_1 \in \mathcal{L}_\infty$ gives that \dot{e}_2 is bounded. Since \dot{e}_3, \dot{e}_5 , and \dot{e}_7 are bounded, we further have that $\dot{\phi}, \dot{\theta}, \dot{\psi} \in \mathcal{L}_\infty$. Consequently, we get $\bar{\tau}_x, \bar{\tau}_y$, and $\bar{\tau}_z$ are bounded which leads to $\ddot{\phi}, \ddot{\theta}, \ddot{\psi} \in \mathcal{L}_\infty$ from the orientation dynamics. Analogous to the aforementioned analysis, we conclude that $\dot{e}_4, \dot{e}_6, \dot{e}_8 \in \mathcal{L}_\infty$.

By observing (48), the boundedness of \ddot{V} implies that \ddot{V} is uniformly continuous. Thus, we have $\lim_{t \rightarrow \infty} \dot{V}(t) = 0$ so as $\lim_{t \rightarrow \infty} e_i(t) = 0$ for $i = 1, \dots, 8$ by invoking Barbalat's Lemma [34]. Therefore, the convergence of the position tracking errors e_1, e_3, e_5, e_7 to the origin demonstrates that the quadrotor system can be guaranteed to go to the desired trajectories. From the definition of e_2, e_4, e_6, e_8 , $\lim_{t \rightarrow \infty} e_i(t) = 0$ for $i = 1, 3, 5, 8$ ensures that $\lim_{t \rightarrow \infty} \dot{e}_i(t) = 0$ for $i = 1, 3, 5, 8$. Consequently, both the position/angle and velocities tracking errors convergent to the origin so that the performance of quadrotor tracking system is proved. \square

3.3 | Velocity control input

In the implementation of the proposed tracking control, the total thrust force F and the net control moments τ are generated from the rotational speed of the four motors. With the proposed adaptive backstepping control, F can be obtained by multiplying mass estimation \hat{m} and nominal force \bar{F} , and similarly for each of the torque τ_x, τ_y , and τ_z . Subsequently, (14) can be utilized with force and torque to obtain the corresponding motor speed. However, the coefficients of lifting force k_F and motor moment k_M , and geometric distance d have to be obtained for the transformation. Most of the previous methods either measures or experimentally derives the coefficients k_F and k_M , but the mismatch of these parameters would degrade the tracking performance and even make the system unstable.

In this section, the proposed adaptive backstepping control is extended to the case by taking into account the lifting and motor coefficients of moment. From the transformation (14), the lifting force with respect to motor speed is given as $F = \sum_{i=1}^4 F_i = \sum_{i=1}^4 k_F \omega_i^2$. By defining $\bar{\omega} := \sum_{i=1}^4 \omega_i^2$, F is rewritten as $F = k_F \bar{\omega}$. With the mass and nominal design, the force input is given as

$$\frac{F}{m} = \frac{k_F}{m} \bar{\omega} := \frac{\bar{\omega}}{m_F}, \quad (49)$$

where $m_F := m/k_F$. Hence, the error dynamics of the subsystem for position tracking (18) becomes

$$\begin{cases} \dot{e}_1 = \dot{\xi}_1 - \dot{\eta}_d = \xi_2 - \eta_d + v_1 - v_1 = e_2 - k_1 e_1 \\ \dot{e}_2 = \dot{\xi}_2 - v_1 = -g a_3 + R a_3 \bar{\omega} / m_F - (\dot{\eta}_d - k_1 \dot{e}_1). \end{cases} \quad (50)$$

By following Steps 1 and 2 in Section 3.1, we consider the augmented Lyapunov function as $V_{2F} = e_1^T e_1 / 2 + e_2^T e_2 / 2 + \tilde{m}_F^2 / (2\gamma_{m_F} m_F)$, where $\tilde{m}_F = m_F - \hat{m}_F$ denotes the estimation error between \hat{m}_F and the actual m_F , which contains both the mass m and the lifting coefficient k_F , and $\gamma_{m_F} \in \mathbb{R}$ is a positive gain for the adaptive law. Therefore, if the nominal velocity input and the adaptive law are designed as

$$\bar{\omega} = -(e_2^T R_f)^{-1} (e_2^T (-g a_3 + \dot{\eta}_d + k_1 \dot{e}_1 + e_1 + k_2 e_2)), \quad (51)$$

$$\dot{\hat{m}}_F = -\gamma_{m_F} \bar{\omega} e_2^T R_f, \quad (52)$$

the position subsystem is stable with $\dot{V}_{2F} = -k_1 e_1^T e_1 - k_2 e_2^T e_2 \leq 0$, so that the position tracking can be ensured.

Similarly, the coefficient of motor moment, k_M , can be considered in the control of three attitude subsystems. The relationships between torque input τ and the motor moment are given as

$$\tau_x = d(F_2 - F_4) = d k_F (\omega_2^2 - \omega_4^2) := d k_F \bar{\omega}_{24}, \quad (53)$$

$$\tau_y = d(F_3 - F_1) = d k_F (\omega_3^2 - \omega_1^2) := d k_F \bar{\omega}_{31}, \quad (54)$$

$$\tau_{\tilde{\zeta}} = \sum_{i=1}^4 (-1)^{i+1} M_i := k_M \bar{\omega}_M, \quad (55)$$

where $\bar{\omega}_{ij} := (\omega_i^2 - \omega_j^2)$ and $\bar{\omega}_M := -\omega_1^2 + \omega_2^2 - \omega_3^2 + \omega_4^2$. Therefore, the torque applied on the x -axis of the quadrotor with the rotational inertia is given as

$$\frac{\tau_x}{I_x} = \frac{dk_F}{I_x} \bar{\omega}_{24} := \frac{\bar{\omega}_{24}}{I_{x\omega}}, \quad (56)$$

where $I_{x\omega} := I_x/dk_F$ and $\bar{\omega}_{24}$ is the nominal velocity input to the moment of x -axis. Subsequently, the error dynamics of the roll angle can be given as

$$\begin{cases} \dot{e}_3 = \dot{\xi}_3 - \dot{\phi}_d = \xi_4 - \dot{\phi}_d + v_3 - v_3 = e_4 - k_3 e_3 \\ \dot{e}_4 = \dot{\xi}_4 - \dot{v}_3 = \rho_{\phi} \xi_6 \xi_8 + \bar{\omega}_{24}/I_{x\omega} - (\ddot{\phi}_d - k_3 \dot{e}_3). \end{cases} \quad (57)$$

By following the analysis in Steps 3 and 4, we have that

$$\bar{\omega}_{24} = -e_3 - k_3 \dot{e}_3 - k_4 e_4 + \ddot{\phi}_d - \hat{\rho}_{\phi} \dot{\theta} \dot{\psi}, \quad (58)$$

$$\dot{\phi}_d = \gamma_{\phi} e_4 \dot{\theta} \dot{\psi}, \quad \dot{I}_{x\omega} = -\gamma_{x\omega} \bar{\omega}_{24} e_4, \quad (59)$$

where $\gamma_{x\omega} \in \mathbb{R}$ is a positive gain of the adaptive law. The nominal velocity input and parameter uncertainties for (54) and (55) are omitted in this section because these control laws can be obtained analogous to the analysis for τ_x and design procedure addressed in Section 3.1.

By observing the modified control and adaptive law for velocity input, we conclude that the proposed algorithms for torque input and velocity input have similar forms. Hence, for the nominal velocity input from the estimated parameters via the adaptive laws, we can obtain from $\bar{\omega}$, $\bar{\omega}_{24}$, $\bar{\omega}_{31}$, and $\bar{\omega}_M$ with the transformation that

$$\begin{bmatrix} \omega_1^2 \\ \omega_2^2 \\ \omega_3^2 \\ \omega_4^2 \end{bmatrix} = \begin{bmatrix} 1 & 1 & 1 & 1 \\ 0 & 1 & 0 & -1 \\ -1 & 0 & 1 & 0 \\ -1 & 1 & -1 & 1 \end{bmatrix}^{-1} \begin{bmatrix} \bar{\omega} \\ \bar{\omega}_{24} \\ \bar{\omega}_{31} \\ \bar{\omega}_M \end{bmatrix}. \quad (60)$$

By following the extension, the uncertainties of kinematics and motor coefficients, d , k_F , and k_M , can be handled simultaneously with the presence of unknown dynamic parameters, m , I_x , I_y , and $I_{\tilde{\zeta}}$.

3.4 | Trajectory generation

Since the quadrotor system with four motor inputs is differentially flat, the control input can be obtained from the algebraic functions of flat outputs that $\{\dot{x}(t), \dot{y}(t), \dot{\zeta}(t), \dot{\psi}(t)\} = \{\eta(t), \psi(t)\}$. The desired trajectories $\{\eta_d(t), \psi_d(t)\}$ of the proposed adaptive backstepping controller can be obtained from

minimum snap trajectory generation [35]. By selecting the desired way-points, we enforce the continuity of the first four derivative of $\eta_d(t)$ and the first two derivatives of $\psi_d(t)$ to generate the feasible trajectories. Thus, $\eta_d(t)$ and $\psi_d(t)$ are twice differentiable as the desired trajectory in the proposed controller.

In addition to $\eta_d(t)$ and $\psi_d(t)$, in the proposed tracking controller the desired trajectories of roll and pitch are required because the rotational inertia is handled separately. Due to the underactuated property, the desired trajectories for roll and pitch angles can not be arbitrarily designed, instead they should be dependent on the desired trajectories $x_d(t)$, $y_d(t)$, $\zeta_d(t)$, and $\psi_d(t)$. Therefore, from the quadrotor dynamics, we denote that $FR_f = [F_x, F_y, F_z]$ as the lifting force in the x - y - ζ direction with respect to the inertial frame W . Consequently, the desired trajectories for the roll and pitch angles are given according to the quadrotor dynamics (8) and (9) as

$$\phi_d(t) = \sin^{-1} \left(\frac{F_x \sin(\psi_d) - F_y \cos(\psi_d)}{F \cos(\theta_d)} \right), \quad (61)$$

$$\theta_d(t) = \sin^{-1} \left(\frac{F_x \cos(\psi_d) + F_y \sin(\psi_d)}{F} \right), \quad (62)$$

which are well-defined as $F(t)$ and $\cos(\theta_d)$ are far from zero.

The resultant desired roll and pitch angles should be twice differentiable for the backstepping controller. Under the assumption of bounds on Euler angles in Section 2, the dependent functions of \sin^{-1} are within the interval $(-1, 1)$. By observing \bar{F} in (40), as \ddot{e}_1 , \dot{e}_2 , and $\ddot{\eta}_d$ are bounded, we get $\bar{F} \in \mathcal{L}_{\infty}$. Since \bar{F} , \dot{e}_2 , $\dot{\phi}$, $\dot{\theta}$, $\dot{\psi} \in \mathcal{L}_{\infty}$, we have that \hat{m} is bounded. Hence, $\dot{F} \in \mathcal{L}_{\infty}$. By taking the time-derivative of the position dynamics in (6), we get $\ddot{\eta}$ being bounded as \dot{F} , $\dot{\phi}$, $\dot{\theta}$, $\dot{\psi} \in \mathcal{L}_{\infty}$. Since $\ddot{\eta}_d$ is bounded, we have that $\ddot{e}_1 \in \mathcal{L}_{\infty}$; additionally, the second derivative of \bar{F} is bounded. We can further obtain that \ddot{F} is bounded from $\ddot{\hat{m}}$ being bounded. Consequently, with fourth differentiable η_d and twice differentiable ψ_d from minimum snap trajectory generation, we conclude that ϕ_d and θ_d addressed in (61) and (62) are twice differentiable.

For the velocity control input studied in Section 3.3, the reference roll and pitch angles can be obtained accordingly with the information of $\ddot{\eta}_d$. As $F/m = \bar{\omega}/m_F$, for the quadrotor to track the desired trajectory η_d and ψ_d , the desired roll and pitch angles can be obtained from (8), (9) that

$$\phi_d(t) = \sin^{-1} \left(\frac{\ddot{x}_d \sin(\psi_d) - \ddot{y}_d \cos(\psi_d)}{\bar{\omega} \cos(\theta_d)} \right), \quad (63)$$

$$\theta_d(t) = \sin^{-1} \left(\frac{\ddot{x}_d \cos(\psi_d) + \ddot{y}_d \sin(\psi_d)}{\bar{\omega}} \right). \quad (64)$$

By utilizing the minimum snap trajectory generation, analogous to (61) and (62), the desired angles (63), (64) are twice differentiable for the implement of the adaptive backstepping controller.

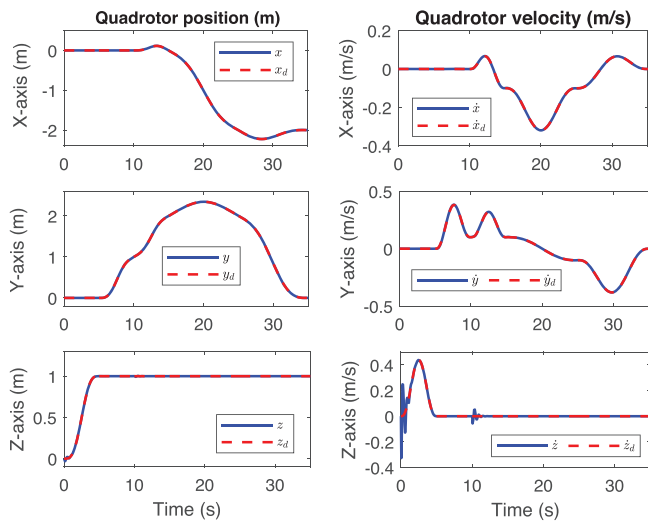


FIGURE 2 Position and velocity tracking in the simulation for a quadrotor to pick up an object in the midway

4 | SIMULATION RESULTS

Numerical examples are illustrated in this section to show the efficacy and efficiency of the proposed adaptive backstepping control algorithm for a quadrotor system with dynamic uncertainties. The minimum snap trajectory generation [35] is utilized to get the feasible trajectory for the quadrotor systems. With the way-points of $x_d = [0, 0, 0, 0, -2, -2] \text{ m}$, $y_d = [0, 0, 1, 2, 2, 0] \text{ m}$, $z_d = [0, 1, 1, 1, 1, 1] \text{ m}$, $\dot{x}_d = [0, 0, 0, -0.1 - 0.10] \text{ m/s}$, $\dot{y}_d = [0, 0, 0.1, 0.1, -0.1, 0] \text{ m/s}$, and $\dot{z}_d = [0, 0, 0, 0, 0, 0] \text{ m/s}$ for $t = [0, 5, 10, 15, 25, 35] \text{ s}$, the desired trajectory can be obtained accordingly. Moreover, the desired yaw angles way-points are given as $\psi_d = [0, 0, \pi/9, 0, \pi/9, 0, \pi/9, 0] \text{ rad}$ for $t = [0, 5, 10, 15, 20, 25, 30, 35] \text{ s}$, and the first and the second derivative of the desired yaw angle are set to zero. During the trajectory tracking, the quadrotor is considered to pick up an object with unknown mass/inertia when $\eta = [0, 1, 1]^T \text{ m}$ at $t = 10 \text{ s}$.

In the simulation, the physical parameters of quadrotor systems are considered as $m = 1 \text{ kg}$, $I_x = 3.2 \times 10^{-3} \text{ kg-m}^2$, $I_y = 3.2 \times 10^{-3} \text{ kg-m}^2$, $I_z = 5 \times 10^{-3} \text{ kg-m}^2$, $k_F = 1.23 \times 10^{-7} \text{ N/rpm}^2$, $k_M = 1.5 \times 10^{-8} \text{ N-m/rpm}^2$, $g = 9.8 \text{ m/s}^2$ and $d = 0.5 \text{ m}$. These parameters are obtained from the DJI F450 quadrotor system, which is utilized in the experimental verification in the next section. In addition to the unknown of m , I_x , I_y , and I_z in the controller, the picked-up object, with 0.2 kg , is also unknown to the controller. For the control gains $k_1 = \text{diag}\{6.10, 6.37, 5.00\}$, $k_2 = \text{diag}\{0.90, 0.63, 2.00\}$, $k_3 = 25$, $k_4 = 10$, $k_5 = 25$, $k_6 = 10$, $k_7 = 6$, $k_8 = 2$, $\gamma_m = 1.5$, and $\gamma_x = \gamma_y = \gamma_z = \gamma_\phi = \gamma_\theta = \gamma_\psi = 1$, the simulation results are shown in Figures 2–4.

The position and velocity tracking performance with the proposed adaptive controller are shown in Figure 2, which illustrates the convergence of the tracking errors in the presence of dynamic uncertainties. The Euler angles and the tracking errors are shown in Figure 3. It shows that the proposed backstepping controller can guarantee the quadrotor system to track

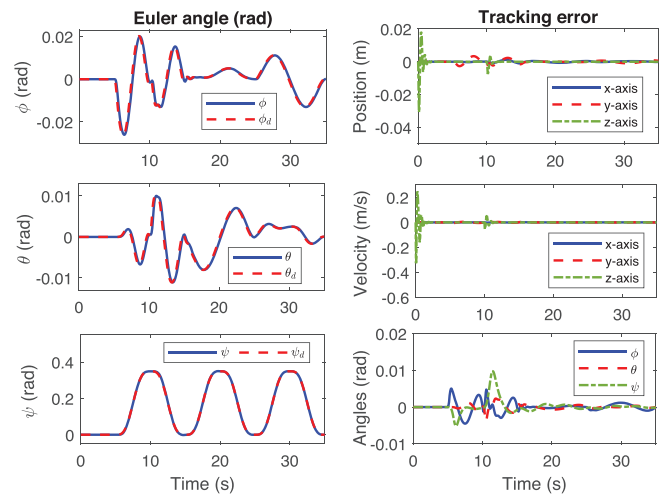


FIGURE 3 Euler angle tracking and errors of the quadrotor system with picking up an object in the midway

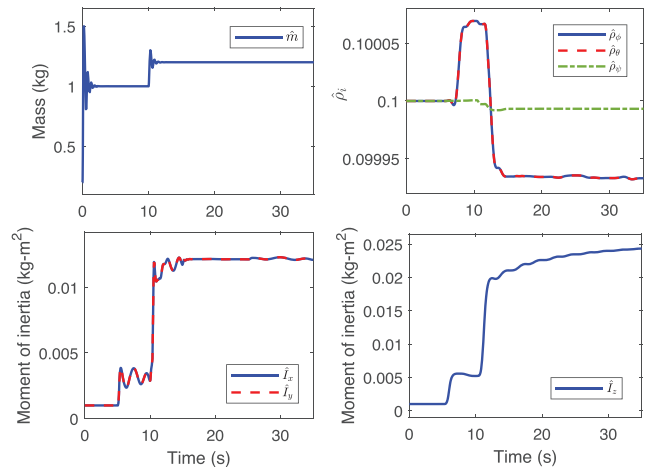


FIGURE 4 Estimates of the unknown dynamic parameters using the proposed adaptive backstepping controller

the desired trajectories; moreover, the tracking of roll, pitch, and yaw angles are ensured for a quadrotor subject to dynamic uncertainties. The estimates of unknown m , ρ_ϕ , ρ_θ , ρ_ψ , I_x , I_y , and I_z are shown in Figure 4. A relative higher variations of \hat{m} is observed in the beginning of the simulation due to the large tracking error in the z -direction. The tracking performance is improved after the convergence of the unknown parameters by utilizing the proposed adaptive law.

The proposed approach is superior to previous algorithms because the mass and rotational inertia are not required in the implementation of the controller. To show the performance of the proposed control scheme, we implement the quadrotor control system under the same scenario by using one of the previously proposed controllers [35]. The controller in [35] is given as

$$F = -k_p e_1 - k_v \dot{e}_1 + mgz + m\ddot{z}_d, \quad (65)$$

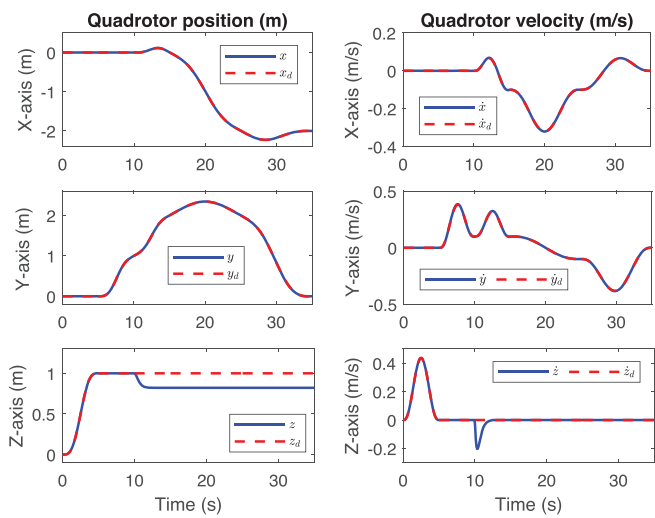


FIGURE 5 Position and velocity tracking in the simulation for a quadrotor to pick up an object in the midway by using a previously proposed controller [35]

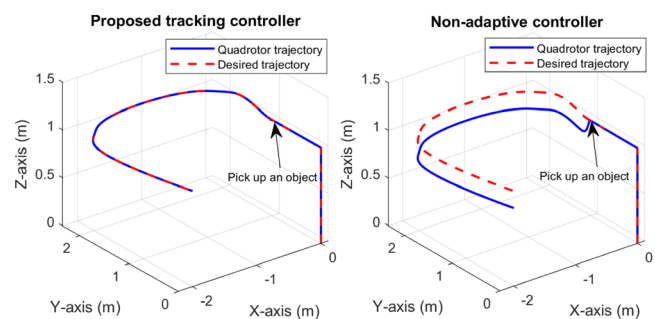


FIGURE 6 Trajectory tracking in 3-D using the proposed controller (left) and the previously developed non-adaptive controller (right) [35]

$$\tau = [\tau_x, \tau_y, \tau_z]^T = -k_r e_r - k_w e_w, \quad (66)$$

where $e_1 = \eta - \eta_d$ is the position tracking error, \dot{e}_1 is the velocity error, e_r is the error on orientation, e_w is the angular velocity error, and k_p, k_v, k_r, k_w are positive control gains. In [35], the controller is considered with perfect knowledge of m and J . Therefore, if the measurement is inaccurate or the mass/inertia change during operation, the controller is unable to guarantee satisfactory tracking performance.

The simulation results of the comparison control algorithm developed in [35] are illustrated in Figure 5. It can be observed that the small oscillation in the beginning of the z -axis velocity does not exist because the dynamic parameters are utilized in the controller. However, when the quadrotor picks up an object with unknown mass at $t = 10$ s, the z -axis velocity has higher variation and the z -axis position drop with a significant tracking error. The trajectory tracking in 3-D for the proposed adaptive controller and the non-adaptive controller are shown in Figure 6. We can conclude that even with suddenly added object to the quadrotor system, the proposed adaptive backstepping controller is superior.

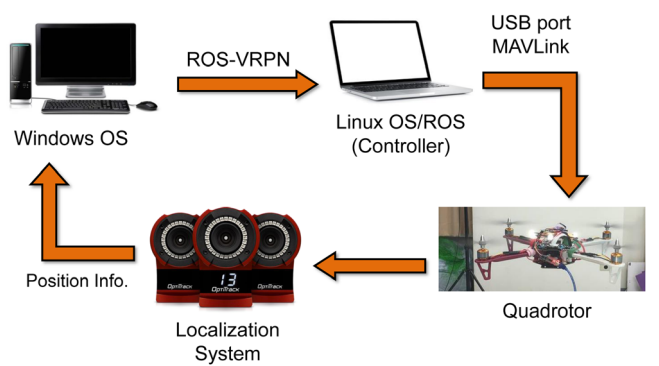


FIGURE 7 Experimental setup for the quadrotor tracking system with the proposed backstepping adaptive controller

5 | EXPERIMENTAL RESULTS

5.1 | Experimental setup

The proposed adaptive backstepping controller is validated in this section via experiments. The quadrotor system is composed of DJI-F450 frame with four A2212-930KV brushless motors. Each of the motor is mounted by a 10-inch propeller with 45° pitch angle. The on-board controller is Pixhawk flight controller with STM32F427Cortex M4, 32bit ARM CortexM4 high performance processor. The experiment setup is illustrated in Figure 7. The position and angle of the quadrotor is acquired by OptiTrack system with the resolution 1280 × 1024 and 120FPS. The delay of the motion capture system is around 8.33ms, and the position information is transmitted to Robot Operating System (ROS) with 100Hz. The controller is implemented in a personal computer (PC), and the control commands are transmitted via ROS to a Linux system and via ROS-MAVLink (Micro Air Vehicle Link) to the Pixhawk on the quadrotor system.

In the experiment, the weight of the quadrotor is 1.195kg, the weight of load platform is 76g, and the weight of the attached object is 100g. Since the flight controller deals with the orientation directly, only the position tracking is implemented and the adaptive mass is considered. In the quadrotor system, the thrust-to-weight ratio is obtained experimentally on all four motors, and the obtained gain is $k_f = 1.28 \times 10^{-7} N/rpm^2$. The control gains for the position tracking are given as $k_1 = diag\{0.9, 1.6, 2.0\}$ and $k_2 = diag\{6.1, 5.4, 5.00\}$. Additionally, in the experiment, the projection operator [36] is utilized with the upper bound and lower bound as $\bar{m} = 1.1kg$ and $\underline{m} = 0.8kg$, respectively. The update rate for the adaptive controller is set as 1.5 for all the following experiments.

5.2 | Trajectory tracking of quadrotor aerial robot

The first experiment presents the tracking performance of the proposed adaptive control for the quadrotor aerial robot. The quadrotor is controlled by using the proposed adaptive backstepping scheme to follow a trajectory generated by the

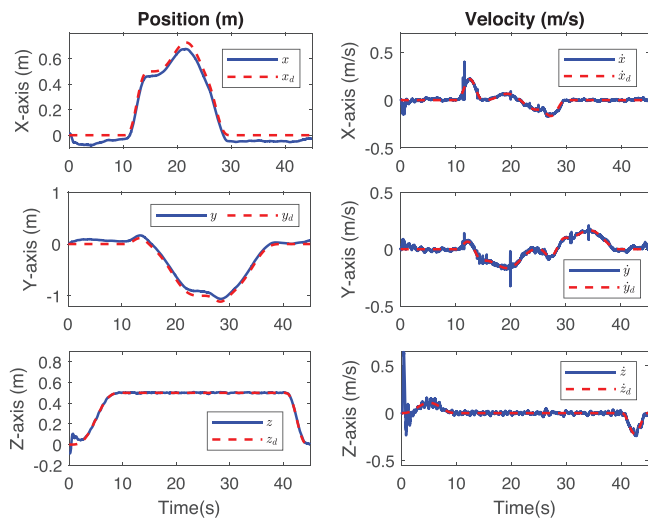


FIGURE 8 Position and velocity tracking in the experiment for a quadrotor to follow a desired trajectory with dynamic uncertainties

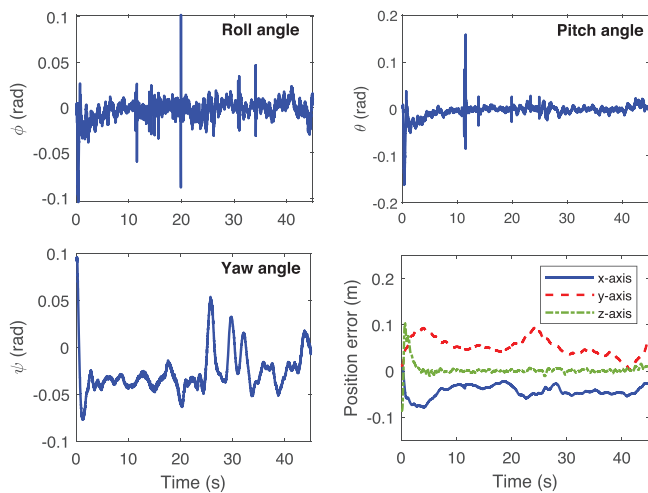


FIGURE 9 Tracking errors of position and Euler angle of the quadrotor system with the use of the proposed adaptive controller

minimum snap algorithm [35]. The trajectory is obtained with the way-points that $x_d = [0, 0.5, 0.5, 0.5, 0, 0, 0] \text{ m}$, $y_d = [0, 0, 0, -1, -1, 0, 0] \text{ m}$, $z_d = [0, 0.5, 0.5, 0.5, 0.5, 0] \text{ m}$ with $\dot{x}_d = [0, 0, 0, -0.1, 0, 0] \text{ m/s}$, $\dot{y}_d = \dot{z}_d = [0, 0, -0.1, 0, -0.1, 0] \text{ m/s}$ for $t = [0, 10, 15, 25, 30, 40, 45] \text{ s}$. The desired yaw angle and angular velocity are set equal to zero for the entire operation.

The experimental results are illustrated in Figures 8–10. As shown in Figure 8, the position and velocity tracking demonstrates that the quadrotor can follow the time-varying trajectory with small and bounded errors. The Euler angles and position tracking errors, as seen in Figure 9, are closed to zero during the operation even if the mass is uncertain in the controller. The 3-D trajectory tracking, motor thrust, and evolution of mass adaption are shown in Figure 10. In the experiment, the position errors mainly result from the ignorance of aerodynamic/propeller effects on the quadrotors.

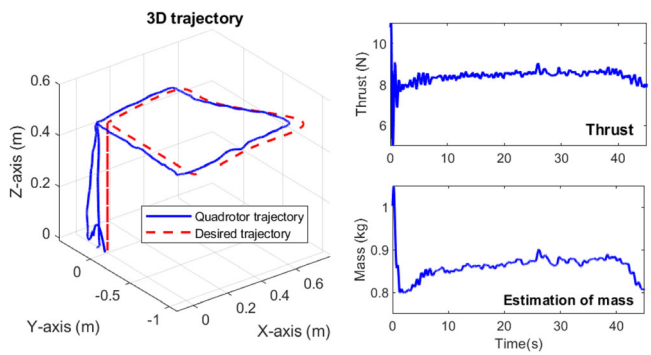


FIGURE 10 Trajectory tracking in 3-D, motor thrust, and estimate of mass in the experiment using the proposed controller

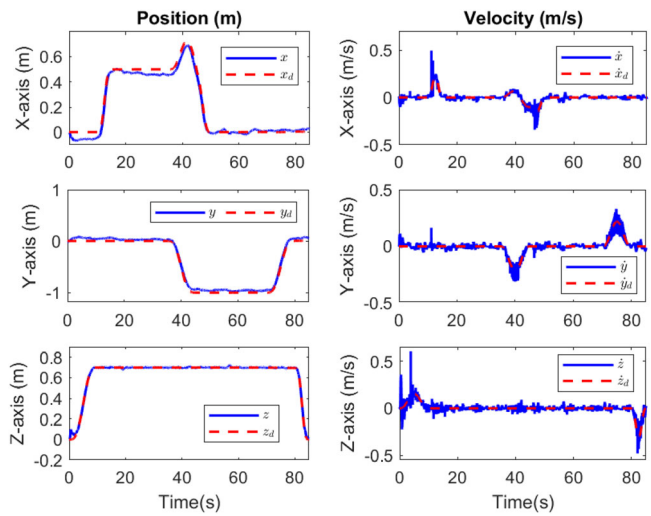


FIGURE 11 Position and velocity tracking in the experiment for a quadrotor to follow a minimum snap trajectory with dynamic uncertainties while added mass in the midway

5.3 | Attaching and detaching objects during tracking

The attaching and detaching mission is important in quadrotor control, and if the dynamic uncertainties are not well-addressed, the quadrotor would fly away or stall. To demonstrate the superiority of the proposed adaptive tracking algorithm, the object is attached to and detached from the quadrotor in the following experiments. First, we consider a minimum snap trajectory which is obtained with the way-points that $x_d = [0, 0, 0.5, 0.5, 0.5, 0, 0, 0] \text{ m}$, $y_d = [0, 0, 0, -1, -1, -1, 0, 0] \text{ m}$, $z_d = [0, 0.7, 0.7, 0.7, 0.7, 0.7, 0, 0] \text{ m}$ with $\dot{x}_d = [0, 0, 0, 0, -0.1, 0, 0, 0] \text{ m/s}$, $\dot{y}_d = \dot{z}_d = [0, 0, 0, 0, 0, 0, 0, 0] \text{ m/s}$ for $t = [0, 10, 15, 35, 45, 50, 70, 80, 85] \text{ s}$. The desired yaw angle and angular velocity are set equal to zero for the entire operation. With the minimum snap trajectory, the quadrotor stops at $\eta = [0.5, 0, 0.7] \text{ m}$ and $\eta = [0, -1, 0.7] \text{ m}$ for 20 s to attach and detach an object to the quadrotor.

The experimental results are shown in Figures 11–14. Figure 11 illustrates that the quadrotor system is able to follow the desired position and velocity. While the object with the

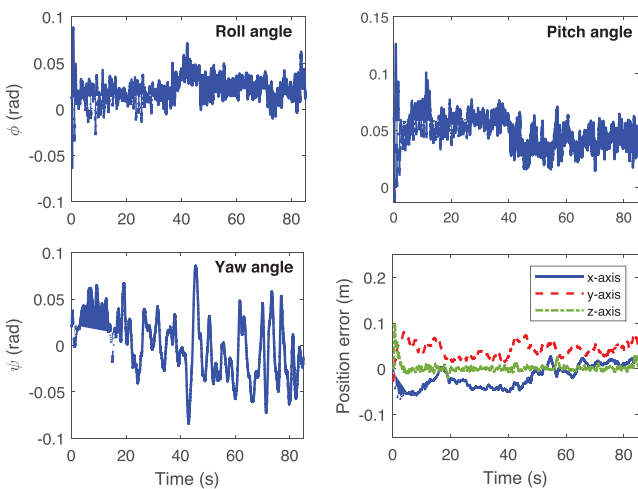


FIGURE 12 Tracking errors of position and Euler angle of the quadrotor system to follow a minimum snap trajectory with the use of the proposed adaptive controller while added mass in the midway

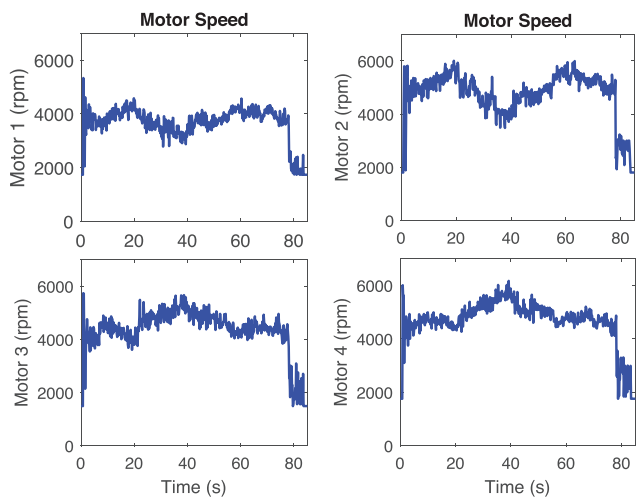


FIGURE 13 Motor speeds of the quadrotor using the proposed controller in minimum snap trajectory

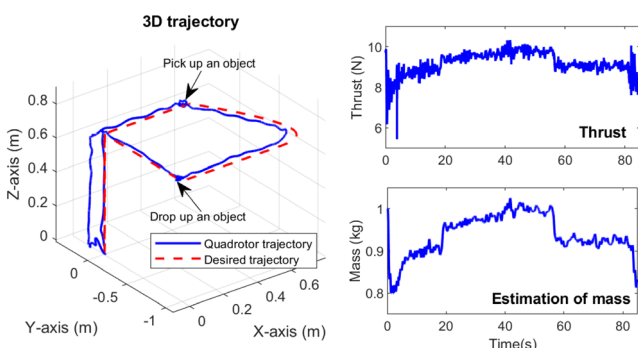


FIGURE 14 Trajectory tracking in 3-D, motor thrust, and estimate of mass in the experiment using the proposed controller to follow a minimum snap trajectory while attaching/detaching mass in the midway

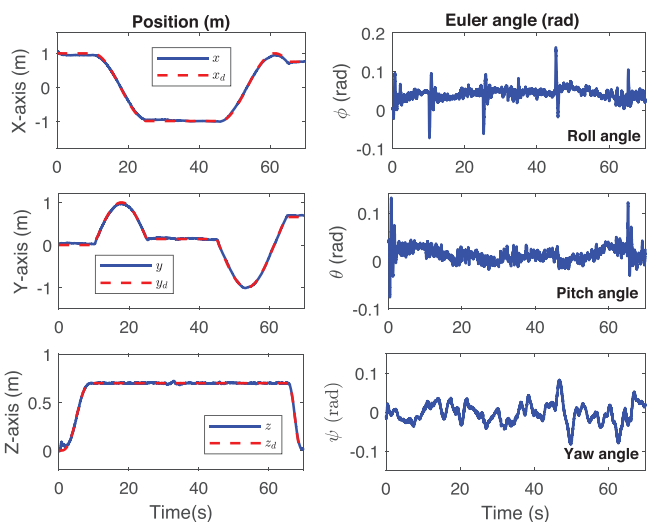


FIGURE 15 Position and angle tracking using the proposed adaptive controller for the quadrotor to track a circle while attaching/detaching object with unknown mass in the midway

mass of 50g is added at around $t = 20$ s and detached from at around $t = 65$ s, the tracking performance is ensured under the change of mass. The tracking of Euler angles and the position tracking errors are illustrated in Figure 12. Additionally, the speeds of the four motors in the quadrotor during operation are shown in Figure 13. The 3-D trajectory tracking is shown in Figure 14, which demonstrates that the quadrotor can follow the desired trajectory independent to dynamic uncertainties. The motor total thrust and estimation of mass are illustrated in Figure 14.

In addition to the desired trajectory generated by minimum snap algorithm, twice differentiable trajectories can also be considered with the proposed adaptive backstepping controller. Next, we consider a circular trajectory given as $x_d(t) = \cos(0.2t)$ and $y_d(t) = \sin(0.2t)$, which satisfies the requirement and assumption of trajectory in Section 3. All the three desired Euler angles are set to equal zero for the entire operation. For the z -axis trajectory, the quadrotor is commanded to flight to $z = 0.7$ m, and keep in this height to follow a circle. Moreover, the quadrotor stops at $t = 25$ s for the operator to attach an object, and keep tracking the circle at $t = 45$ s until $t = 70$ s for landing. The experimental results are shown in Figures 16 and 17, where the convergence of position and Euler angles errors to the origin are guaranteed. Bounded position tracking errors and estimation of mass with suddenly attached mass demonstrate the efficacy of the proposed controller.

6 | CONCLUSIONS

The knowledge of accurate mass/inertia is extremely important to guarantee high efficient and performance for quadrotor aerial robots on trajectory tracking. In the previous studies, the perfect

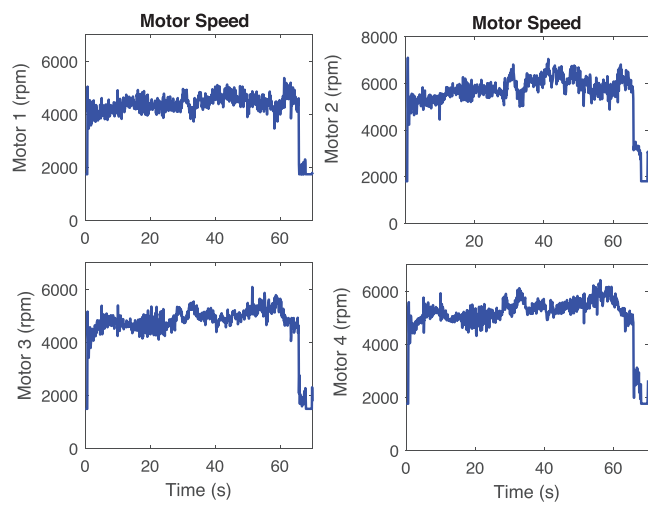


FIGURE 16 Motor speed of the quadrotor using the proposed controller in circular trajectory

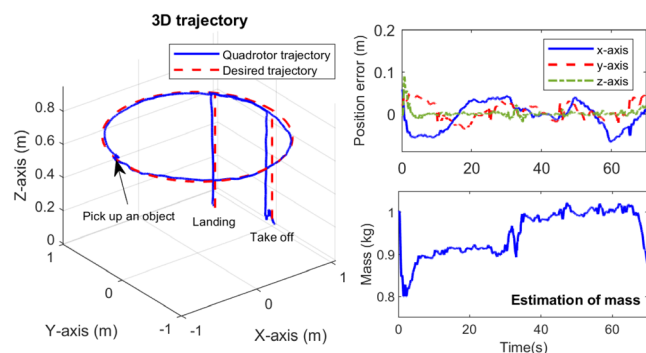


FIGURE 17 3-D tracking, position tracking error, and estimate of mass of the quadrotor system tracking a circle while attaching/detaching object with unknown mass in the midway

knowledge of m and J are required to ensure satisfactory tracking; however, the precise measurements on mass/inertia are difficult to achieve. Especially, when there are unknown objects attached to or detached from a quadrotor during operation, the aerial system could be unstable or fly away/stall if the uncertain dynamic parameters are not well-copied within the design of controller. This paper studies an adaptive tracking control for non-linear quadrotor systems subject to parameter uncertainties with the technique of backstepping control.

To ensure both stability and tracking performance, the proposed adaptive backstepping control can guarantee a quadrotor system to track a time-varying trajectory in the presence of dynamic uncertainties. With the concept of nominal inputs, the force and torque commands to the quadrotor is decoupled with the uncertain physical parameters. Subsequently, a design procedure for four subsystems of a quadrotor is proposed with the design of adaptive laws to estimate the mass and inertia during operation. The stability and convergence of tracking errors to the origin are studied by utilizing Lyapunov theorem. Additionally, the presence of unknown motor coefficient and geometric parameter can also be tackled by the proposed nominal input

and adaptive laws. Numerical examples and experiments are illustrated to demonstrate the efficiency of the adaptive quadrotor tracking systems.

Although the control performance is guaranteed and demonstrated in the numerical examples, the aerodynamic/propeller effects would significant influence the tracking performance in practice, as seen in the experimental results. Therefore, it is necessary to consider the presence of disturbances and aerodynamic effects as the extensions of this work. Additionally, the future work of this research topic could also encompass the study of transporting a cable-suspended object without the knowledge of object dynamics.

ACKNOWLEDGEMENTS

This work was supported in part by the Ministry of Science and Technology (MOST), Taiwan, under grants MOST 108-2636-E-006-007 and MOST 109-2636-E-006-019.

REFERENCES

- Ruggiero, F., Lippiello, V., Ollero, A.: Aerial manipulation: a literature review. *IEEE Rob. Autom. Lett.* 3(3), 1957–1964 (2018)
- Lee, T.: Geometric control of quadrotor UAVs transporting a cable-suspended rigid body. *IEEE Trans. Control Syst. Technol.* 26(1), 255–264 (2018)
- Mahony, R., Kumar, V., Corke, P.: Multirotor aerial vehicles: Modeling, estimation, and control of quadrotor. *IEEE Rob. Autom. Mag.* 19(3), 56–65 (2012)
- Kuo, C.-W., Tsai, C.-C.: Quaternion-based adaptive backstepping RFWNN control of quadrotors subject to model uncertainties and disturbances. *Int. J. Fuzzy Syst.* 20(6), 1745–1755 (2018)
- Michael, N., Mellinger, D., Lindsey, Q., Kumar, V.: The grasp multiple micro-UAV testbed. *IEEE Rob. Autom. Mag.* 17(3), 56–65 (2010)
- Lei, W., Li, C., Chen, M. Z. Q.: Robust adaptive tracking control for quadrotors by combining PI and self-tuning regulator. *IEEE Trans. Control Syst. Technol.* 27(6), 2663–2671 (2019)
- Huang, M., Xian, B., Diao, C., Yang, K., Feng, Y.: Adaptive tracking control of underactuated quadrotor unmanned aerial vehicles via backstepping. In: Proceedings of the American Control Conference, Baltimore (2010)
- Zuo, Z.: Trajectory tracking control design with command-filtered compensation for a quadrotor. *IET Control Theory Appl.* 4(11), 2343–2355 (2010)
- Tayebi, A., McGilvray, S.: Attitude stabilization of a vtol quadrotor aircraft. *IEEE Trans. Control Syst. Technol.* 14(3), 562–571 (2006)
- Freddi, A., Lanzon, A., Longhi, S.: A feedback linearization approach to fault tolerance in quadrotor vehicles. In: Proceedings of the 18th World Congress, Milano (2011)
- Ryan, T., Kim, H.J.: Lmi-based gain synthesis for simple robust quadrotor control. *IEEE Trans. Autom. Sci. Eng.* 10(4), 1173–1178 (2013)
- Alexis, K., an dA Tzes, G.N.: Model predictive quadrotor control: Attitude, altitude and position experimental studies. *IET Control Theory Appl.* 6(12), 1812–1827 (2012)
- Abdollahi, T., Salehfar, S., Xiong, C.-H., Ying, J.-F.: Simplified fuzzy-pade controller for attitude control of quadrotor helicopters. *IET Control Theory Appl.* 12(2), 310–317 (2018)
- Chen, F., Jiang, R., Zhang, K., Jiang, B., Tao, G.: Robust backstepping sliding-mode control and observer-based fault estimation for a quadrotor UAV. *IEEE Trans. Ind. Electron.* 63(8), 5044–5056 (2016)
- Madani, T., Benallegue, A.: Control of a quadrotor mini-helicopter via full state backstepping technique. In: IEEE Conference on Decision and Control (CDC), San Diego (2006)
- Ramirez-Rodriguez, H., Parra-Vega, V., Sanchez-Orta, A., and Garcia-Salazar, O.: Robust backstepping control based on integral sliding modes for tracking of quadrotors. *J. Intell. Rob. Syst.* 73, 51–66 (2014)

17. Chen, F., Lei, W., Zhang, K., Tao, G., Jiang, B.: A novel nonlinear resilient control for a quadrotor UAV via backstepping control and nonlinear disturbance observer. *Nonlinear Dyn.* 85(2), 1281–1295 (2016)
18. Ou, T.-W., Liu, Y.-C.: Adaptive backstepping tracking control for quadrotor aerial robots subject to uncertain dynamics. In: American Control Conference, Philadelphia (2019)
19. Madani, T., Benallegue, A.: Backstepping control with exact 2-sliding mode estimation for a quadrotor unmanned aerial vehicle. In: IEEE/RSJ International Conference on Intelligent Robots and Systems, San Diego (2007)
20. Liu, H., Zhao, W., Hong, S., Lewis, F.L., and Yu, Y.: Robust backstepping-based trajectory tracking control for quadrotors with time delays. *IET Control Theory Appl.* 13(12), 1945–1954 (2019)
21. Lu, H., Liu, C., Coombes, M., Guo, L., Chen, W.-H.: Online optimisation-based backstepping control design with application to quadrotor. *IET Control Theory Appl.* 10(14), 1601–1611 (2016)
22. Fresk, E., Nikolakopoulos, G.: A generalized frame adaptive MPC for the low-level control of UAVs. In: European Control Conference, Limassol (2018)
23. Madani, T., Benallegue, A.: Adaptive control via backstepping technique and neural networks of a quadrotor helicopter. In: IFAC World Congress, Seoul (2008)
24. Lee, D., Nataraj, C., Burg, T., Dawson, D.M.: Adaptive tracking control of an underactuated aerial vehicle. In: American Control Conference, San Francisco (2011)
25. Zou, Y.: Trajectory tracking controller for quadrotors without velocity and angular velocity measurements. *IET Control Theory Appl.* 11(1), 101–109 (2017)
26. Choi, Y.-C., Ahn, H.-S.: Nonlinear control of quadrotor for point tracking: Actual implementation and experimental tests. *IEEE/ASME Trans. Mechatron.* 20(3), 1179–1192 (2015)
27. Kaya, D., Kutay, A.T.: Aerodynamic modeling and parameter estimation of a quadrotor helicopter. In: AIAA Atmospheric Flight Mechanics Conference, Atlanta (2014)
28. Yang, S., Xian, B.: Exponential regulation control of a quadrotor unmanned aerial vehicle with a suspended payload. *IEEE Trans. Control Syst. Technol.* 28(6), 2762–2769 (2019)
29. Poultnay, A., Gong, P., Ashrafiou, H.: Integral backstepping control for trajectory and yaw motion tracking of quadrotors. *Robotica* 37(2), 300–320 (2019)
30. Wang, R., Liu, J.: Trajectory tracking control of a 6-DOF quadrotor UAV with input saturation via backstepping. *J. Franklin Inst.* 355(7), 3288–3309 (2018)
31. Poultnay, A., Kennedy, C., Clayton, G., Ashrafiou, H.: Robust tracking control of quadrotors based on differential flatness: simulations and experiments. *IEEE/ASME Trans. Mechatron.* 23(3), 1126–1137 (2018)
32. Xu, R., U. Özgüner: Sliding mode control of a class of underactuated systems. *Automatica* 44, 233–241 (2008)
33. Zhou, J., Wen, C.: Adaptive Backstepping Control of Uncertain Systems: Nonsmooth Nonlinearities, Interactions or Time-variations. Springer, New York (2008)
34. Khalil, H.K.: Nonlinear Systems. Prentice Hall, New Jersey (2002)
35. Mellinger, D., Kumar, V.: Minimum snap trajectory generation and control for quadrotors. In: IEEE International Conference on Robotics and Automation, Shanghai (2011)
36. Liu, Y.-C., Khong, M.-H.: Adaptive control for nonlinear teleoperators with uncertain kinematics and dynamics. *IEEE/ASME Trans. Mechatron.* 20(5), 2550–2562 (2015)

How to cite this article: Liu Y-C, Ou T-W. Non-linear adaptive tracking control for quadrotor aerial robots under uncertain dynamics. *IET Control Theory Appl.* 2021;15:1126–1139.
<https://doi.org/10.1049/cth2.12112>